Inorganic Chemistry

Article

pubs.acs.org/IC

Highly Ag^+ Selective Tripodal Gold(I) Acetylide-based "Off–On" Luminescence Chemosensors based on $^3(\pi\pi^*)$ Emission Switching

Yu-Peng Zhou, En-Bao Liu, Jin Wang, and Hsiu-Yi Chao*

MOE Key Laboratory of Bioinorganic and Synthetic Chemistry, School of Chemistry and Chemical Engineering, Sun Yat–Sen University, Guangzhou 510275, P. R. China

Supporting Information

ABSTRACT: Newly prepared gold(I) acetylide-based luminescent cation sensors **1c** and **1d**, which bear a novel three–armed flexible conformation, together with control molecule **2c**, were synthesized in four steps. **1c** and **1d** exhibit the $\pi \rightarrow \pi^*$ absorption of the acetylide ligands in fluid solutions and produce the $^3(\pi\pi^*)$ emission of the acetylide ligands in the solid state and degassed THF solution. The $^3(\pi\pi^*)$ emission of **1c** in DMSO can be turned on upon addition of Ag^+. The binding ratio between **1c** and Ag^+ as well as the binding constant log K were determined as 1:1 and 4.35 ± 0.12 respectively by UV–vis titration experiments. The formation of $[\mathbf{1c}\cdot Ag]^+$ adduct, which leads to the appearance of new up-field peaks, was confirmed by ^{1}H NMR spectroscopic titrations. The control ^{1}H NMR titration experiments for the acetylide-free analogue **1a** and single-armed analogue **2c** indicate the acetylide groups and tripodal structures are responsible for the binding of Ag^+. The control experiment for tripodal gold(I) acetylide analogue **1d** suggests the change of PPh_3 with $P(2\text{-}Py)Ph_2$ induces similar binding affinity toward Ag^+ but less selectivity toward Ag^+. Free **1c** also exhibits the anion binding affinity toward F^-, but the Ag^+ adduct $[\mathbf{1c}\cdot Ag]^+$ shows less affinity toward F^-.

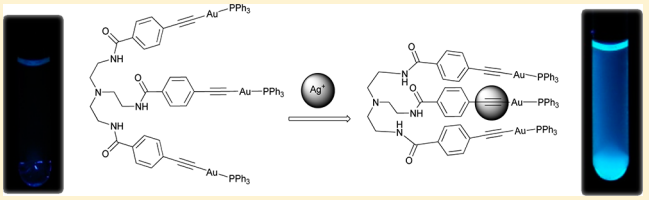

INTRODUCTION

The design of chemosensors is important as they are in great demand in the areas of analytical and clinical chemistry, environmental science, and medicine.[1] Among the potential sensing targets, heavy transition-metal ions have attracted significant attention because widespread issues such as environmental pollution pose serious problems, especially in developing countries.[2] Ag^+ is one of the most critical ions since it can form covalent, colloidal, and coordination bonds with various natural ligands and present significant toxicity as well as problematic detectability requiring better probe modalities.[3] Current instrumental methods for detecting metal ions such as FAAS, GFAAS, ICP–AES, and ICP–MS have been developed. They are sufficient, mature, and in wide use, but these methods involve expensive and intricate instrumentation and careful operation. Thus, reliable and efficient methods for detecting metal ions using optically reporting chemosensors are required.[4] Over the past years, certain Ag^+ sensors based on organic molecules,[5a–e] metal complexes,[5f] QDs,[6] nanoparticles,[7] and DNA/oligonucleotides[8] have been reported. Among these, various sensors based on novel metal complexation modes have attracted much attention because they have controllable geometries, large Stokes shifts, and long lifetimes.[9] For luminescent metal complexes, gold(I) complexes are an important class that facilitate a triplet excited state emission; relativistic effects allow for the formation of weak Au···Au interactions.[10] The studies of photophysics,[11] supramolecular building,[12] and chemosensors[13] based on Au···Au interactions and gold(I) complexes have been reported. Among these, gold(I) acetylide complexes bearing the unsaturated organic C≡C motif that allows strong $^3(\pi\pi^*)$ emission facilitated through the "heavy atom effect" is quite important. Structure–property relationships of $^3(\pi\pi^*)$ luminescence[14] have been reported by Che and co-workers and show the interesting and various photophysical properties of gold(I) acetylide complexes.

Compared to the traditional binding units toward Ag^+, such as cyclic or acyclic N, O, S donor ligands,[4] phthalocyanine,[5g] and aromatic π-electrons,[15] the use of acetylide Ag^+ binding groups is less explored. Yam and co-workers have reported that Ag^+ can interact with acetylide groups to perturb its emission property in the solid state[16] and act as a photoswitch toward the photoisomerization of the host molecule.[17] The Ag^+ and acetylide π-electron interactions have also been illustrated in the crystal structures of some metal acetylide complexes.[18] These results encouraged us to use the acetylide group in Ag^+ binding, a motif previously used in NLO materials, liquid crystals, and molecular wires.[19]

To extend our previous work on the photophysical and ion-sensing properties of gold(I) acetylide complexes,[13a,14d,e] tripodal gold(I) acetylide sensors **1c** and **1d** (Scheme 1) were prepared, derived from *tris*(2-aminoethyl)amine (*tren*), a widely used building block in anion encapsulation,[20] anion sensing,[21] and anion transportation.[22] The Au σ-bonded acetylide group usually involves the $^3(\pi\pi^*)$ emissive excited

Received: March 31, 2013

   dx.doi.org/10.1021/ic400791a | *Inorg. Chem.* XXXX, XXX, XXX–XXX

Scheme 1. (a) Chemical Structures of 1c, 1d, and 2c and (b) Proposed Binding Model between 1c and Ag^+

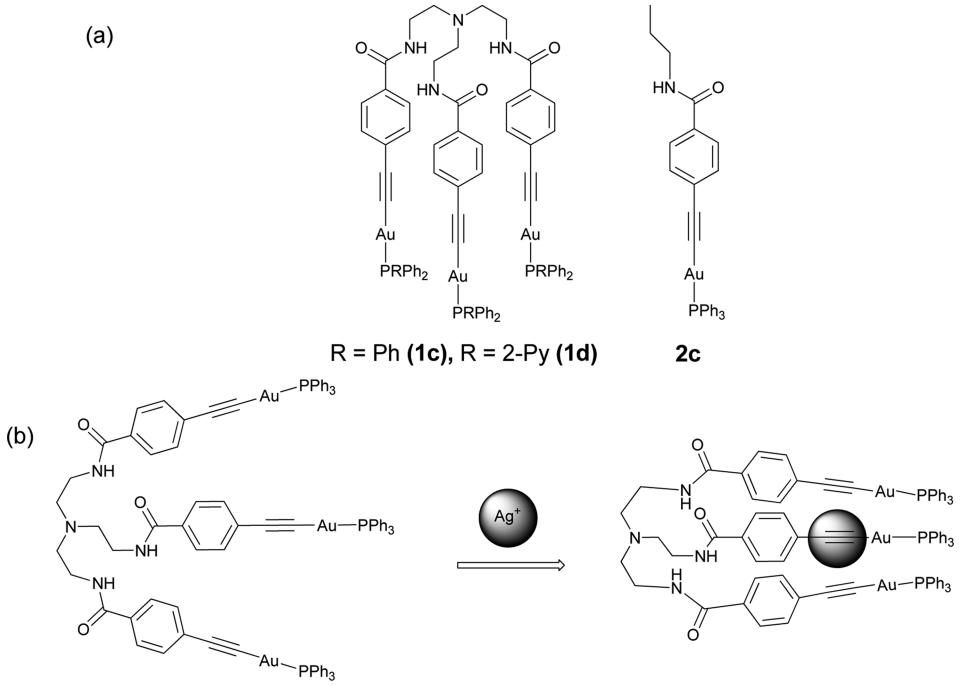

state of similar gold(I) acetylide complexes, which provides the possibility to perturb the luminescent properties upon binding of Ag^+. The flexible tripodal structure, compared to linear or cyclic forms, allows for conformational changes upon ion binding, which may cause the three arms close to each other and increase the possibility to form intramolecular Au···Au interactions among three Au atoms attaching on each arm. In this work, we report the synthesis, photophysical properties, and ion-sensing ability of tripodal-based gold(I) acetylide complexes **1c** and **1d**. The silver ion-sensing mechanism of **1c** has also been studied. For comparison, the mononuclear gold(I) acetylide complex (**2c**) was synthesized (Scheme 1).

EXPERIMENTAL SECTION

Materials and Reagents. Au(THT)Cl was synthesized according to literature procedures.[23] Tris(2-aminoethyl)amine and 4-iodobenzoyl chloride were purchased from Alfa-Aesar. Trimethylsilylacetylene, *n*-propylamine, diphenyl-2-pyridylphosphine, and triphenylphosphine were obtained from J & K. Silver nitrate, copper(I) bromide, lead nitrate, zinc nitrate hexahydrate, copper(II) nitrate trihydrate, nickel(II) nitrate hexahydrate, cobalt(II) nitrate hexahydrate, cadmium nitrate tetrahydrate, aluminum nitrate nonahydrate, calcium nitrate tetrahydrate, magnesium nitrate hexahydrate, potassium nitrate, and sodium nitrate were purchased from Aladdin. Tetra-*n*-butylammonium fluoride hydrate, tetra-*n*-butylammonium chloride hydrate, tetra-*n*-butylammonium bromide, tetra-*n*-butylammonium iodide, tetra-*n*-butylammonium acetate, and tetra-*n*-butylammonium phosphate were obtained from Sigma-Aldrich.

Synthesis of $N(CH_2CH_2NHC(O)C_6H_4\text{-}4\text{-}I)_3$ (1a). To a suspension of 4-iodobenzoyl chloride (1.2 g, 4.5 mmol) in anhydrous CH_2Cl_2 (30 mL), tris(2-aminoethyl)amine (219 mg, 1.5 mmol) and NEt_3 (1 mL) in CH_2Cl_2 (5 mL) were added dropwise. The mixture was stirred at room temperature overnight under nitrogen. The solvent was removed under reduced pressure, and the residue was washed with hydrochloric acid and dilute sodium hydroxide solution, respectively. The white solid was collected and washed with water. Yield: 690 mg, 55%. ^1H NMR (300 MHz, DMSO-d_6, 298 K): δ = 8.30 (t, J = 5 Hz, 3 H, N−H), 7.70 (d, J = 8 Hz, 6 H, $-C_6H_4-$), 7.48 (d, J = 8 Hz, 6 H, $-C_6H_4-$), 3.33 (m, 6 H, $-CH_2-$), 2.67 (t, J = 6 Hz, 6 H, $-CH_2-$). IR (KBr, cm^{-1}): ν = 3300 (N−H), 1633 (C═O). ESI−MS: m/z = 835 $[M - H]^-$. Anal. Calcd for $C_{27}H_{27}N_4O_3I_3$ (%): C, 38.79; H, 3.25; N, 6.70. Found: C, 38.97; H, 3.19; N, 6.74.

Synthesis of $N(CH_2CH_2NHC(O)C_6H_4\text{-}4\text{-}C{\equiv}C{-}TMS)_3$ (1b). To a mixture of **1a** (627 mg, 0.75 mmol), CuI (40 mg, 0.20 mmol), and $Pd(PPh_3)_2Cl_2$ (50 mg, 0.07) in THF (20 mL), trimethylsilylacetylene (330 mg, 3.4 mmol) and $NHEt_2$ (2 mL) were added dropwise, respectively. The mixture was stirred at room temperature under nitrogen overnight. The solvent was removed under reduced pressure, and the residue was purified by column chromatography on alumina (elute: first, CH_2Cl_2, followed by EA/MeOH, (9:1 v/v)). The product was obtained as a brown solid. Yield: 226 mg, 40%. ^1H NMR (300 MHz, DMSO-d_6, 298 K): δ = 8.39 (t, J = 5 Hz, 3 H, N−H), 7.74 (d, J = 8 Hz, 6 H, $-C_6H_4-$), 7.44 (d, J = 8 Hz, 6 H, $-C_6H_4-$), 3.34 (m, 6 H, $-CH_2-$), 2.69 (t, J = 6 Hz, 6 H, $-CH_2-$), 0.25 (s, 27 H, $Si(CH_3)_3$). IR (KBr, cm^{-1}): ν = 3305 (N−H), 2159 (C≡C), 1634 (C═O). ESI−MS: m/z = 745 $[M - H]^-$. Anal. Calcd for $C_{42}H_{54}N_4Si_3O_3{\cdot}0.2C_4H_8O{\cdot}0.2H_2O$ (%): C, 67.18; H, 7.38; N, 7.32. Found: C, 67.45; H, 7.66; N, 7.23.

Synthesis of $[N(CH_2CH_2NHC(O)C_6H_4\text{-}4\text{-}C{\equiv}CAu)_3]_\infty$ (polymer 1). To a mixture of **1b** (22 mg, 0.03 mmol) and Au(THT)Cl (29 mg, 0.09 mmol) in CH_2Cl_2 (10 mL), excess KF (17 mg, 0.18 mmol) in MeOH (2 mL) was added dropwise. The mixture was stirred at room temperature for 30 min in the dark. The dark brown precipitate was collected and reacted with triphenylphosphine directly in the next reaction. Caution: the gold(I) acetylide polymer is potentially explosive.[24]

Synthesis of $N(CH_2CH_2NHC(O)C_6H_4\text{-}4\text{-}C{\equiv}CAuPPh_3)_3$ (1c). To the suspension of **polymer 1** in CH_2Cl_2 (20 mL), triphenylphosphine (24 mg, 0.09 mmol) was added. The mixture was stirred overnight in the dark. After filtration, the filtrate was concentrated and *n*-hexane was added to form the light yellow precipitate. The precipitate was collected and dried in vacuum. Yield: 48 mg, 82%. ^1H NMR (300 MHz, DMSO-d_6, 298 K): δ = 8.34 (t, J = 5 Hz, 3 H, N−H), 7.71 (d, J = 8 Hz, 6 H, $-C_6H_4-$), 7.58−7.50 (m, 45H, phenyl), 7.30 (d, J = 8 Hz, 6 H, $-C_6H_4-$), 3.35 (m, 6 H, $-CH_2-$), 2.69 (t, J = 6 Hz, 6 H, $-CH_2-$). ^{31}P NMR (121 MHz, DMSO-d_6, 298 K): δ = 42.40. IR (KBr, cm^{-1}): ν = 3263 (N−H), 2111 (C≡C), 1646 (C═O). ESI−MS: m/z = 1905 $[M+H]^+$. Anal. Calcd for $C_{87}H_{72}Au_3N_4O_3P_3{\cdot}H_2O$ (%): C, 54.33; H, 3.88; N, 2.91. Found: C, 54.23; H, 3.95; N, 3.03.

dx.doi.org/10.1021/ic400791a | Inorg. Chem. XXXX, XXX, XXX−XXX

Scheme 2. Synthetic Route of 1c and 1d[a]

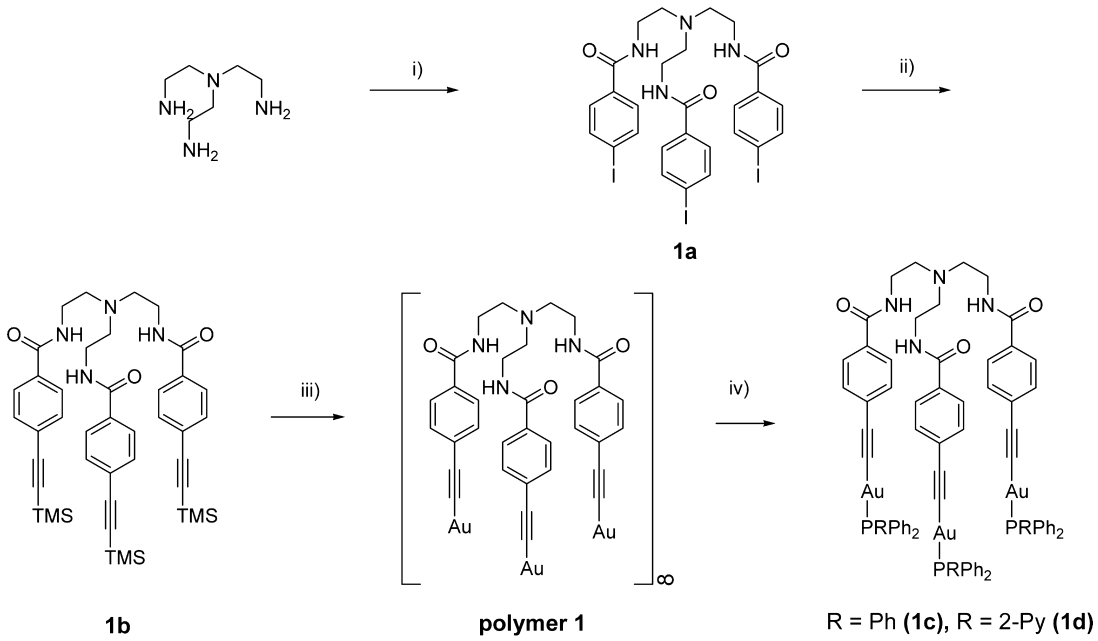

[a](i) 4-iodobenzoyl chloride, CH_2Cl_2, NEt_3, RT, overnight. (ii) TMS−C≡CH, $Pd(PPh_3)_2Cl_2$, CuI, $NHEt_2$, THF, RT, overnight. (iii) Au(THT)Cl, KF, MeOH/CH_2Cl_2, RT, 0.5 h, dark. (iv) PPh_3 or P(2-Py)Ph_2, CH_2Cl_2, RT, overnight, dark.

Synthesis of $N(CH_2CH_2NHC(O)C_6H_4\text{-}4\text{-}C{\equiv}CAuP(2\text{-}Py)Ph_2)_3$ (1d). To the suspension of polymer **1** in CH_2Cl_2 (20 mL), diphenyl-2-pyridylphosphine (26 mg, 0.10 mmol) was added. The mixture was stirred at room temperature overnight in the dark. After filtration, the filtrate was concentrated and *n*-hexane was added to form the pale-yellow precipitate. The precipitate was collected and dried in vacuum. Yield: 38 mg, 60%. ^{1}H NMR (300 MHz, DMSO-d_6, 298 K): δ = 8.77 (d, J = 5 Hz, 3 H, Py), 8.38 (t, J = 5 Hz, 3 H, N−H), 7.91 (m, 3 H, Py), 7.71 (d, J = 8 Hz, 6 H, $-C_6H_4-$), 7.62−7.48 (m, 36H, phenyl and Py), 7.34 (d, J = 8 Hz, 6 H, $-C_6H_4-$), 3.36 (m, 6 H, $-CH_2-$), 2.69 (m, 6 H, $-CH_2-$). ^{31}P NMR (121 MHz, DMSO-d_6, 298 K): δ = 41.70. IR (KBr, cm^{-1}): ν = 3336 (N−H), 2108 (C≡C), 1643 (C═O). ESI−MS: m/z = 1908 $[M + H]^+$. Anal. Calcd for $C_{84}H_{69}Au_3N_7O_3P_3{\cdot}H_2O$ (%): C, 52.37; H, 3.72; N, 5.09. Found: C, 52.56; H, 4.02; N, 4.99.

Synthesis of $CH_3CH_2CH_2NHC(O)C_6H_4\text{-}4\text{-}I$ (2a). To a suspension of 4-iodobenzoyl chloride (1.07 g, 4.0 mmol) in CH_2Cl_2 (20 mL), *n*-propylamine (2 mL) was added dropwise. The mixture was stirred at room temperature for 20 min. The solvent was removed under reduced pressure, and the residue was washed with water and dilute NaOH solution. The white solid was collected and washed with dilute hydrochloric acid and water. Yield: 823 mg, 71%. ^{1}H NMR (300 z, $CDCl_3$, 298 K): δ = 7.76 (d, J = 8 Hz, 2 H, $-C_6H_4-$), 7.46 (d, J = 8 Hz, 2 H, $-C_6H_4-$), 6.06 (s, 1 H, N−H), 3.40 (m, 2 H, $-CH_2-$), 1.63 (m, 2 H, $-CH_2-$), 0.98 (t, J = 7 Hz, 3 H, $-CH_3$). IR (KBr, cm^{-1}): ν = 3311 (N−H), 1631 (C═O). EI−MS: m/z = 289 $[M]^+$. Anal. Calcd for $C_{10}H_{12}INO$ (%): C, 41.54; H, 4.18; N, 4.84. Found: C, 41.81; H, 4.26; N, 4.83.

Synthesis of $CH_3CH_2CH_2NHC(O)C_6H_4\text{-}4\text{-}C{\equiv}C{-}TMS$ (2b). To a mixture of **2a** (289 mg, 1.0 mmol), CuI (20 mg, 0.11 mmol), and $Pd(PPh_3)_2Cl_2$ (30 mg, 0.04 mmol) in THF (10 mL) and NEt_3 (10 mL), trimethylsilylacetylene (150 mg, 1.5 mmol) was added dropwise. The mixture was stirred overnight at room temperature under nitrogen. The solvent was removed under reduced pressure, and the residue was purified by column chromatography on silica gel (elute: first CH_2Cl_2, followed by EA). The product was obtained as a brown solid. Yield: 191 mg, 74%. ^{1}H NMR (300 MHz, $CDCl_3$, 298 K): δ = 7.67 (d, J = 8 Hz, 2 H, $-C_6H_4-$), 7.49 (d, J = 8 Hz, 2 H, $-C_6H_4-$), 6.08 (s, 1 H, N−H), 3.41 (m, 2 H, $-CH_2-$), 1.64 (m, 2 H, $-CH_2-$), 0.99 (t, J = 7 Hz, 3 H, $-CH_3$), 0.26 (s, 9 H, $Si(CH_3)_3$). IR (KBr, cm^{-1}): ν = 3256 (N−H), 2160 (C≡C), 1626 (C═O). ESI−MS: m/z = 260 $[M + H]^+$. Anal. Calcd for $C_{15}H_{21}NOSi$ (%): C, 69.45; H, 8.16; N, 5.40. Found: C, 69.43; H, 8.27; N, 5.17.

Synthesis of $[CH_3CH_2CH_2NHC(O)C_6H_4\text{-}4\text{-}C{\equiv}CAu]_\infty$ (polymer 2). To a mixture of **2b** (26 mg, 0.10 mmol) and Au(THT)Cl (32 mg, 0.10 mmol) in CH_2Cl_2 (10 mL), excess KF (19 mg, 0.20 mmol) in MeOH (1 mL) was added dropwise. The mixture was stirred at room temperature for 30 min in the dark. The dark brown precipitate was collected and reacted with triphenylphosphine directly in the next reaction. **Caution**: the gold(I) acetylide polymer is potentially explosive.

Synthesis of $CH_3CH_2CH_2NHC(O)C_6H_4\text{-}4\text{-}C{\equiv}CAuPPh_3$ (2c). To the suspension of **polymer 2** in CH_2Cl_2 (20 mL), triphenylphosphine (26 mg, 0.10 mmol) was added. The mixture was stirred at room temperature overnight in the dark. After filtration, the filtrate was concentrated and *n*-hexane was added to form the gray precipitate. The precipitate was collected and dried in vacuum. Yield: 37 mg, 57%. ^{1}H NMR (300 MHz, DMSO-d_6, 298 K): δ = 8.38 (t, J = 5 Hz, 1 H, N−H), 7.73 (d, J = 8 Hz, 2 H, $-C_6H_4-$), 7.62−7.48 (m, 15H, Phenyl), 7.35 (d, J = 8 Hz, 2 H, $-C_6H_4-$), 3.19 (m, 2 H, $-CH_2-$), 1.51 (m, 2 H, $-CH_2-$), 0.88 (t, J = 7 Hz, 3 H, $-CH_3$). ^{31}P NMR (121 MHz, DMSO-d_6, 298 K): δ = 42.41. IR (KBr, cm^{-1}): ν = 3263 (N−H), 2123 (C≡C), 1631 (C═O). FAB−MS: m/z = 646 $[M + H]^+$. Anal. Calcd for $C_{30}H_{27}AuNOP{\cdot}0.2H_2O$ (%): C, 55.51; H, 4.25; N, 2.16. Found: C, 55.49; H, 4.17; N, 2.04.

Physical Measurements and Instrumentation. Chemical shifts (δ, ppm) were reported relative to tetramethylsilane for ^{1}H NMR, 85% H_3PO_4 for ^{31}P NMR on a Varian Mercury-Plus 300 spectrometer. Infrared spectra were recorded from KBr pellets in the range of 400−4000 cm^{-1} on a Bruker-EQUINOX 55 FT−IR spectrometer. Electrospray ionization (ESI) mass spectra were recorded on a LCQ DECA XP quadrupole ion trap mass spectrometer. Fast atom bombardment (FAB) mass spectra were recorded on a Thermo MAT95XP high resolution mass spectrometer. Electron impact (EI) mass spectra were recorded on a Thermo DSQ mass spectrometer. Elemental analysis was performed on Elemental Vario EL elemental analyzer. Electronic absorption spectra were measured on a PGENERAL TU1901 UV−vis spectrophotometer. Emission spectra were obtained on a FLSP920 fluorescence spectrophotometer.

dx.doi.org/10.1021/ic400791a | Inorg. Chem. XXXX, XXX, XXX−XXX

Titrations, Job Plots, and Detection Limit. For the typical UV−vis and emission titration experiments, 1.5 μL aliquots of a nitrate salt were added into the 3 mL solution of the complex in DMSO by a syringe, and the spectral changes were recorded by a PGENERAL TU1901 UV−vis spectrophotometer and FLSP920 fluorescence spectrophotometer at 298 K. The volume changes after the addition of ions were kept less than 5% (150 μL). For a typical ^{1}H NMR titration experiment, 1.0 μL aliquots of a nitrate salt were added into the 0.5 mL solution of the complex in DMSO-d_6 by syringe, and the ^{1}H NMR spectral changes were recorded by a Varian Mercury-Plus 300 spectrometer at 298 K. The binding constant log K values were determined by nonlinear fitting using a 1:1 binding model.[25a] Job plots were obtained from a series of solutions in which the fraction of the corresponding anions varied, keeping the total concentration (the complexes and cations) constant. The maxima of the plots indicated the binding stoichiometry of the complexes with cations. Detection limit was determined by FLSP920 fluorescence spectrophotometer at 298 K when S(signal)/N(noise) = 3.3.[25b]

RESULTS AND DISCUSSION

Synthesis and Characterization. The synthetic route of **1c** and **1d** involves four steps that all bear satisfactory yields (Scheme 2). First, *tris*(2-aminoethyl)amine (*tren*) reacted with 4-iodobenzoyl chloride in 1:3 ratio to form an insoluble intermediate **1a** in CH_2Cl_2. Second, through Sonogashira coupling reaction, the iodine groups of **1a** were substituted by acetylide groups to obtain the better solubility intermediate **1b** used to react with three equivalents of Au(THT)Cl[23] in the presence of excess KF to form the gold(I) acetylide **polymer 1** (caution: the gold(I) acetylide polymer is potentially explosive[24]). Finally, three equivalents of phosphine ligands were added into the suspension of **polymer 1** in CH_2Cl_2 to depolymerize **polymer 1** to get the final products **1c** and **1d** respectively (the attempts to get other pure derivatives with alkyl substituted phosphine ligands were not successful). The procedure for the synthesis of mononuclear analogue **2c** is similar to those for **1c** and **1d** (Scheme S1, Supporting Information). Complexes **1c**, **1d**, and **2c** are all air-stable at 298 K and were characterized by IR, ^{1}H, and ^{31}P NMR spectroscopy as well as mass spectrometry (ESI, EI, or FAB) and elemental analysis.

The IR spectra of complexes **1c**, **1d**, and **2c** reveal three bands at ca. 3263−3336, 2108−2123, and 1631−1646 cm^{-1}, characteristic of the stretches of ν(N−H), ν(C≡C), and ν(C═O), respectively. The ^{1}H NMR spectra of complexes **1c**, **1d**, and **2c** show a triplet peak centered at 8.34−8.38 ppm, respectively, which comes from the resonances of the protons of N−H. The peaks appeared at ca. 7.30−7.73 ppm can be ascribed to the resonances of protons coming from the aromatic phenyl rings. The upfield multiplet signals at the range of ca. 0.88−3.36 ppm come from the alkyl protons. The ^{31}P NMR spectra of **1c**, **1d**, and **2c** display singlets at 41.70−42.41 ppm, similar to those of the previously reported gold(I) acetylide complexes with triphenylphosphine.[13a] Well-defined $[M + H]^+$ peaks of complexes **1c**, **1d**, and **2c** were observed through the positive charge ESI and FAB mass spectrometry.

Photophysics Studies. The electronic absorption spectrum of **1c** in DMSO at 298 K shows the absorption maxima at ca. 260, 292, and 305 nm with shoulders at ca. 270, 275, and 324 nm, which undergo bathochromic shifting, compared with the free ligand **1b** (Figure S1a and Table S1, Supporting Information). The vibrational progressional spacings of ca. 1500 and 2000 cm^{-1} ascribed to the symmetric phenyl ring stretching and ν(C≡C) stretches, respectively, are observed. The electronic absorption bands of **1d** and **2c** are similar to those of **1c**, but the molar absorptivity of **2c** is smaller than that of **1c** (Figure S1 and Table S1, Supporting Information). Thus, the absorption bands of **1c**, **1d**, and **2c** at 260−327 nm are assigned to the $\pi \rightarrow \pi^*$ transition of the acetylide ligands. The electronic absorption spectra of **1c** as well as **2c** in THF at 298 K are very similar to those in DMSO, which may suggest the solvents have a little effect on the electronic absorption spectra (Table S1, Supporting Information).

Excitation of **1c** and **1d** in the solid state and degassed THF at λ_{ex} > 300 nm at 298 K produces the blue-green emission with a μs range lifetime. For the solid state emission spectra of **1c** and **1d**, the observed vibrational spacings of ca. 1100 and 2000 cm^{-1} in 472−554 nm (Table S1 and Figure S2, Supporting Information) are attributed to the stretches of phenyl rings deformation and ν(C≡C), respectively. The emission spectrum of **1c** and **1d** in degassed THF (Table S1 and Figure S3, Supporting Information) also reveals the bands at ca. 410−510 nm and 450−555 nm respectively with the vibrational spacings of ca. 1100, 1600, and 2100 cm^{-1}, which are ascribed to the stretches of phenyl rings deformation, ν(C═O), and ν(C≡C), respectively. These spectra are spaced similar to those of previously reported gold(I) acetylide complexes, suggesting that the lowest lying emissive state of **1c** and **1d** for 410−555 nm emission bands may come from the acetylide-based $^3(\pi\pi^*)$ excited state promoted by the enhanced intersystem crossing through the "heavy atom effect" of Au that increases spin-orbit coupling.[13a,14] In contrast, in DMSO solutions of **1c** and **1d** (degassed or not degassed), the background emission bands of DMSO appear at ca. 350−450 nm; the $^3(\pi\pi^*)$ emission bands expected at λ > 450 nm are difficult to observe.

Cation Sensing studies. The cation-sensing properties of **1c** have been investigated by titration experiments in DMSO (upon addition of Ag^+ into the THF solution of **1c**, the precipitate was formed. Thus, the titration experiments in THF were not tested). Common cations were screened (nitrates were used); some cations such as Hg^{2+} and Fe^{3+} have limited solubility in DMSO. Upon addition of Ag^+ into the DMSO solution of **1c** (5.0×10^{-5} mol dm^{-3}, λ_{ex} = 311 nm), the emission intensity at 472 nm increases dramatically together with the color change of the luminescence: from blue-violet (emission from DMSO solvent) to blue-green (Figure 1). Thus, the emission at 472 nm switches on with an

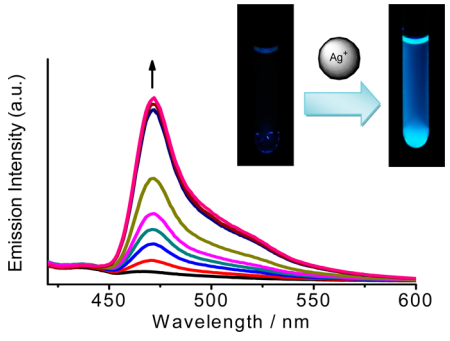

Figure 1. Emission spectral changes of **1c** (5.0×10^{-5} mol dm^{-3}, λ_{ex} = 311 nm) in DMSO upon addition of Ag^+ (the emission bands at λ < 450 nm come from the emission of DMSO solvent). (Inset) Photographs of **1c** in DMSO without (left) and with Ag^+ (right) under the excitation of 365 nm irradiation.

dx.doi.org/10.1021/ic400791a | Inorg. Chem. XXXX, XXX, XXX−XXX

enhancement of ca. 18-fold. The binding constant (log K) of **1c** with Ag^+ in DMSO, determined via luminescence titration, is 4.56 ± 0.21 (Figure S4, Supporting Information), which is in accord to that obtained by UV−vis titration data (*vide infra*). The detection limit for Ag^+ is estimated to be 1.0×10^{-6} mol dm^{-3} (Figure S5, Supporting Information). For comparison, a control luminescence titration experiment of the single-arm analogue **2c** was carried out with Ag^+ (Figure S6, Supporting Information). Upon addition of Ag^+, the emission band at ca. 470 nm reveals extremely small enhancement compared with that for **1c**. This result suggests that the single acetylide arm very weakly interacts with Ag^+ and multi-armed acetylide groups may play an essential role in Ag^+ binding (Scheme 1b).

The selectivity of **1c** in DMSO toward other metal ions has been investigated. The emission spectra of **1c** (5.0×10^{-5} mol dm^{-3}, λ_{ex} = 311 nm) after the addition of two equivalents of various metal ions were recorded (Figure S7, Supporting Information). Except Ag^+, other metal ions studies in this work cannot turn on the emission at 472 nm (Figure 2, row a). Ag^+ concentration creates the ca. 18-fold emission intensity increase at 472 nm, suggesting the remarkable responsiveness of **1c** toward Ag^+.

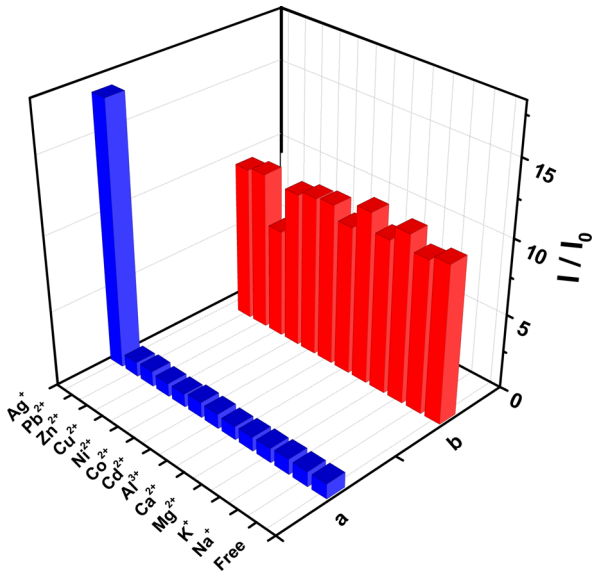

Figure 2. (Row a) Relative emission intensity at 472 nm of **1c** (5.0×10^{-5} mol dm^{-3}, λ_{ex} = 311 nm) with 2 equiv of various metal ions. (Row b) Relative emission intensity at 472 nm of **1c** (5.0×10^{-5} mol dm^{-3}, λ_{ex} = 311 nm) + 1 equiv Ag^+ in the presence of various metal ions (2 equiv for Cu^{2+}; 10 equiv for Na^+, K^+, Ca^{2+}, and Al^{3+}; 5 equiv for others).

In addition, the competitive binding experiments of **1c** toward Ag^+ in the presence of competitive concentrations of other metal ions (5−10 fold) have been carried out. The emission spectra of **1c** (5.0×10^{-5} mol dm^{-3}, λ_{ex} = 311 nm) with one equivalent of Ag^+ in the presence of various metal ions were recorded. In the presence of less than 10 equivalents of Na^+, K^+, Ca^{2+}, and Al^{3+}, the influence on the emission intensity at 472 nm is small; in the presence of less than 5 equivalents of Pb^{2+}, Zn^{2+}, Ni^{2+}, Co^{2+}, Cd^{2+}, and Mg^{2+}, the emission intensity at 472 nm changes a little (Figure 2, row b). The metal ion that only affects the sensing is Cu^{2+}, suggesting reasonable selectivity of **1c** toward Ag^+. The luminescence intensity at 472 nm decreases ca. 30% in the presence of more than 2 equiv of Cu^{2+}, suggesting its effective quenching effect. These results indicate that Ag^+ is highly competitive to bind **1c** in the presence of various metal ions studied in this work other than Cu^{2+}.

Mechanism Studies for Cation Sensing. In order to understand the mechanism for the interaction of **1c** with Ag^+, UV−vis and ^1H NMR spectral titration experiments were carried out. The UV−vis spectral changes of **1c** (5×10^{-6} mol dm^{-3}) in DMSO upon addition of Ag^+ are shown in Figure 3a. The absorption bands at 292 and 305 nm decrease gradually whereas the absorbances at ca. 261 and 345 nm increase gradually upon addition of Ag^+. Well-defined isosbestic points are observed at 274 and 311 nm, verifying direct cation-complex adduct formation. In terms of specificity, other metal ions studied in this work did not produce such spectral changes.

To further investigate the binding ratio between Ag^+ and **1c**, Job analysis was carried out. The UV−vis spectra of continuous variation with Ag^+ were recorded in DMSO ([**1c**] + [Ag^+] = 5×10^{-5} mol dm^{-3}). The absorptions of the newly formed band at 355 nm reveal their maximum when [Ag^+]/([Ag^+] + [**1c**]) reaches at ca. 0.5 (Figure 3b), supporting 1:1 stoichiometric Ag^+−**1c** binding. Using nonlinear fitting and a 1:1 binding model, the binding constant log K' (UV−vis titration) was determined to be 4.35 ± 0.12 (Figure 3a inset), in accordance with the log K (luminescence titration) obtained before.

Figure 4 contains ^1H NMR spectra reflecting clear changes upon addition of Ag^+ into **1c** (1.0 mmol dm^{-3}) in DMSO-d_6. The bottom one shows the spectrum of **1c** in the absence of Ag^+. The triplet signal centered at 8.34 ppm, doublets signals centered at 7.71 and 7.30 ppm, and the multiplet signal at 7.50−7.58 ppm are attributed to the protons of the N−H (H_A), $-C_6H_4-$ (H_B, H_C, respectively), and phenyl rings of triphenylphosphine moieties, respectively. Upon addition of Ag^+ gradually, the intensities of signals centered at 8.34 ppm (J = 5.0 Hz), 7.71 ppm (J = 8.2 Hz) and 7.30 ppm (J = 8.2 Hz) decrease. Meanwhile, a triplet centered at ca. 7.47 ppm (J = 5.1 Hz) and doublets centered at 7.12 ppm (J = 8.1 Hz) and 6.88 ppm (J = 8.0 Hz) gradually rise evenly from the baseline. At the same time, the multiplet signal at 7.50−7.58 ppm changes from multiple to single gradually. Signals centered at ca. 7.30 (H_C), 7.71 (H_B), and 8.34 ppm (H_A) disappear completely when the amount of Ag^+ is larger than one equivalent, supporting saturative behavior with a stoichiometric amount of analyte. The pattern and coupling constants of newly formed peaks appear closely related to those of disappearing peaks, suggesting they may come from the [**1c**·Ag^+] adduct. Upon addition of Ag^+, **1c** transfers to [**1c**·Ag^+] gradually (unfortunately, the attempt to characterize the [**1c**·Ag^+] adduct by ESI−MS was not successful). It is interesting to note these spectral changes differ from many host−guest systems whose NMR spectral signals usually shift gradually upfield or downfield. The upfield positions of the newly formed peaks here could be explained as the formation of "closed clamp" conformation upon Ag^+ binding that makes the N−H as well as $-C_6H_4-$ motifs of three arms proximal and leads to a dramatic increase of electronic density which introduces enhanced shielding that causes the signals to appear upfield.

The reversibility of the binding of **1c** with Ag^+ has been tested. The ^1H NMR spectra upon addition of Cl^-, Br^-, and I^- into the DMSO-d_6 solution of **1c** in the presence of one equivalent of Ag^+ were recorded. Figures S8−S10 (Supporting Information) show spectral changes that **1c** undergoes (1.0 mmol dm^{-3}) with one equivalent of Ag^+ upon addition of Cl^-,

dx.doi.org/10.1021/ic400791a | Inorg. Chem. XXXX, XXX, XXX−XXX

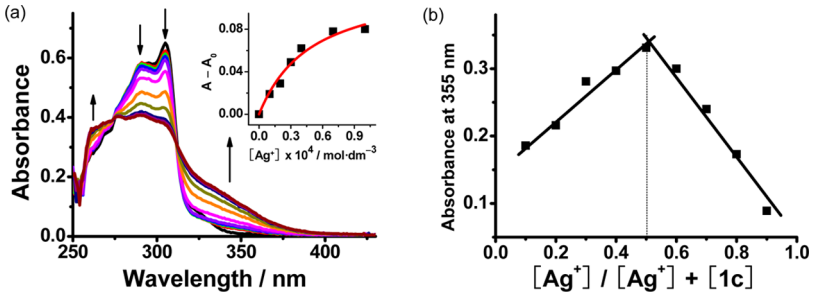

Figure 3. (a) UV−vis spectral changes of **1c** (5.0×10^{-6} mol dm^{-3}) in DMSO upon addition of Ag^+. (Inset) Plot of the absorbance change at 355 nm as a function of the concentration of Ag^+ and a 1:1 theoretical fitting of the data. (b) Job's plot of complex **1c** with Ag^+ in DMSO ([**1c**] + [Ag^+] = 5×10^{-5} mol dm^{-3}).

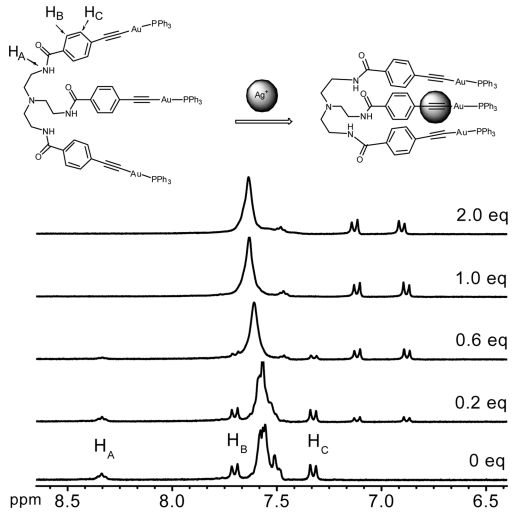

Figure 4. ^{1}H NMR spectral changes of **1c** (1.0 mmol dm^{-3}) in DMSO-d_6 upon addition of Ag^+.

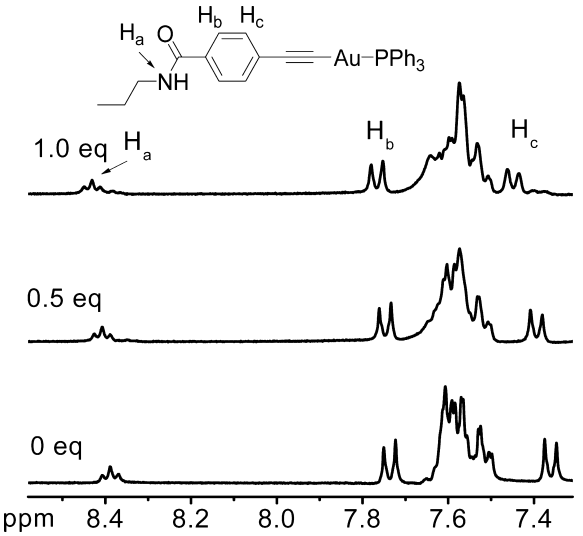

Figure 5. ^{1}H NMR spectral changes of **2c** (4 mmol dm^{-3}) in DMSO-d_6 upon addition of Ag^+.

Br^-, and I^- (n-Bu_4N salts), respectively (DMSO-d_6). The sharp signal at 7.61 ppm, which comes from the phenyl ring protons of PPh_3, undergoes an upfield shift. The triplet centered at ca. 7.47 ppm and doublets centered at 7.12 ppm and 6.88 ppm show minimal shifting, indicating the "closed clamp" conformation of [**1c**·Ag^+] is consistent, and the binding between **1c** and Ag^+ is irreversible in DMSO in the presence of halides strongly favored by Ag^+ binding.

As a control experiment, the ^{1}H NMR spectral titration of the single-armed analogue **2c** with Ag^+ was carried out. Figure 5 reveals the spectral changes of **2c** (4.0 mmol dm^{-3}) in DMSO-d_6 upon addition of Ag^+. The triplet centered at 8.38 ppm, doublets centered at 7.73 and 7.35 ppm, and the multiplet centered at 7.48−7.62 ppm are attributed to protons of the N−H (H_a), $-C_6H_4-$ (H_b, H_c, respectively), and P-phenyl ring protons, respectively. Upon addition of Ag^+ gradually, the changes of signals centered at 8.38 ppm (H_a) and 7.73 ppm (H_b) can be barely observed. The signal centered at 7.35 ppm (H_c) shows slight downfield shifting. This could be due to the interaction between Ag^+ and acetylide group of **2c** that reduces the electron density of the adjacent protons of $-C_6H_4-$ motif (H_c). The signals at 7.48−7.62 ppm also show a small change in their patterns. Thus, the spectral changes of single-armed analogue **2c** are quite different from those of three-armed sensor **1c**, suggestive of the notion that a three-armed flexible conformation produces better hosting of Ag^+.

In the literature, N, O, and π-electrons of aromatic rings can be used as binding units toward Ag^+.[4,14] In order to confirm the binding units of **1c** with Ag^+, the ^{1}H NMR spectroscopic titration of **1a** in DMSO-d_6 with Ag^+ was also performed (Figure S11, Supporting Information). The ^{1}H NMR spectrum of **1a** without any Ag^+ has the triplet centered at 8.30 ppm and doublets centered at 7.70 and 7.48 ppm, attributed to N−H, $-C_6H_4-$ motifs, respectively. Upon addition of two equivalents of Ag^+, the ^{1}H NMR spectral changes are very small. This may suggest that the binding units of **1c** with Ag^+ do not involve the nitrogen atoms or π-electrons of phenyl rings. Thus, three C≡C moieties of **1c** are corresponded to Ag^+ binding.

The influence of phosphine ligand P(2-Py)Ph_2 of the tripodal gold(I) acetylide complex **1d** on Ag^+ binding was investigated by luminescence, UV−vis, and NMR titration experiments, which are shown in Figures S12−S18 (Supporting Information). They all have similar spectral changes compared with those of **1c**. The binding constants log K_{1d} with Ag^+ were determined to be 4.62 ± 0.24 (luminescence) and 4.42 ± 0.10 (UV−vis), which are close to those of **1c**. However, for the selectivity of **1d** with cations, Cu^{2+} leads to the slight enhancement of emission intensity, which could be rationalized as the binding of Cu^{2+} on pyridine N atom (Figure S14, Supporting Information). Thus, the change of R group with pyridine moiety does not affect the affinity toward Ag^+ but decreases the selectivity for Ag^+.

It is interesting to compare the cation-sensing mechanism of gold(I) acetylide complex **1c** with that of other gold(I) acetylide complexes previously reported by Yam, in which the

dx.doi.org/10.1021/ic400791a | Inorg. Chem. XXXX, XXX, XXX−XXX

emission based on intramolecular Au···Au interaction could be produced at λ_{em} > 550 nm.[13c,f,g] The emission band of **1c** at 472 nm in DMSO solution, which can also be found in those of free **1c** in the solid state and degassed THF solution, was switched on when **1c** binds Ag^+. Figure S19 (Supporting Information) shows the emission spectra of free **1c** in degassed THF solution and **1c** in the presence of two equivalents of Ag^+ in DMSO solution. The maximum peaks and shoulder peaks agree with each other very well. The lifetime of maximum band of **1c** upon addition of Ag^+ in DMSO was determined as 4.4 μs. Thus, the acetylide-based $^3(\pi\pi^*)$ emission could be turned on when **1c** interacts with Ag^+ in DMSO solution. The very weakly emission of **1c** at 472 nm in DMSO could be due to the solvent effect of DMSO, which may reduce the radiative decay of the triplet excited state. Upon addition of Ag^+, the interaction between acetylide groups and the Ag^+ may facilitate spin−orbit coupling and thus enhance the radiative decay of the triplet excited state. In addition, when **1c** binds Ag^+, the intra- and/or intermolecular aurophilic interactions may produce the rigidity, which could increase the emission intensity. As a control experiment, the titration experiment of **1c** toward Cu^+ was carried out (CuBr was used because it is more stable than $[Cu(CH_3CN)_4]PF_6$ in air). Upon addition of Cu^+ into the DMSO solution of **1c** (5×10^{-5} mol dm^{-3}), the intensity of the emission band at 525 nm increases (λ_{ex} = 311 nm) (Figure S20, Supporting Information). Meanwhile, the intensity of the emission band at 472 nm also increases, but the enhancement is small compared with that of 525 nm emission band and that of 472 nm emission band upon addition of Ag^+ (Figures S20 and S21, Supporting Information). The excitation spectra of **1c** with 4 equivalents of Cu^+ and Ag^+ in DMSO are shown in Figure S22 (Supporting Information). The excitation spectrum of **1c** with Cu^+ (λ_{em} = 525 nm) shows a low energy band at ca. 400 nm, which is in accord to appearance of the new absorption band at 400 nm in the UV−vis titration experiment (Figure S23, Supporting Information) and is absent in the excitation spectrum of **1c** with Ag^+ (λ_{em} = 472 nm). Thus, the emission band at 525 nm is attributed to come from the excited state associated with Au···Au interactions when **1c** binds Cu^+ in DMSO. As a control experiment, the emission and ^{1}H NMR spectra of $AuPPh_3$-free ligand **1b** upon addition of Ag^+ do not change, indicating the essential role of $AuPPh_3$ motifs during the sensing process (Figures S24 and S25, Supporting Information).

Anion Binding Studies. Derivates of *tris*(2-aminoethyl)-amine (*tren*) have been used widely for anion recognition.[20−22] Thus, the anion binding properties of **1c** were also investigated by ^{1}H NMR spectroscopic titrations. Figure 6 shows the ^{1}H NMR spectral changes of **1c** (1.0 mmol dm^{-3}) in DMSO-d_6 upon addition of F^-. The triplet peak centered at 8.34 ppm assigned to N−H undergoes gradual downfield shifting (after one equivalent of F^- was added, the peak of N−H became very broad and its intensity became weak), which suggests the existence of N−H···F^- hydrogen bonding. The signal of H_B coming from the $-C_6H_4-$ motif which is close to the N−H motif shows a comparably large downfield shift understood as the increased polarization effect of C−H bond introduced by the through-space effect.[13a,26] Another proton signal H_C originating from the $-C_6H_4-$ motif greatly distal from the N−H shows very little shifting, indicating the weak influence to H_C. The titration experiments of **1c** with other anions (Cl^-, $H_2PO_4^-$, and OAc^-) have also been carried out. The spectral changes are quite small (see Figures S26−S28, Supporting Information), showing the relatively weak interactions compared with previously reported organic analogues.[27]

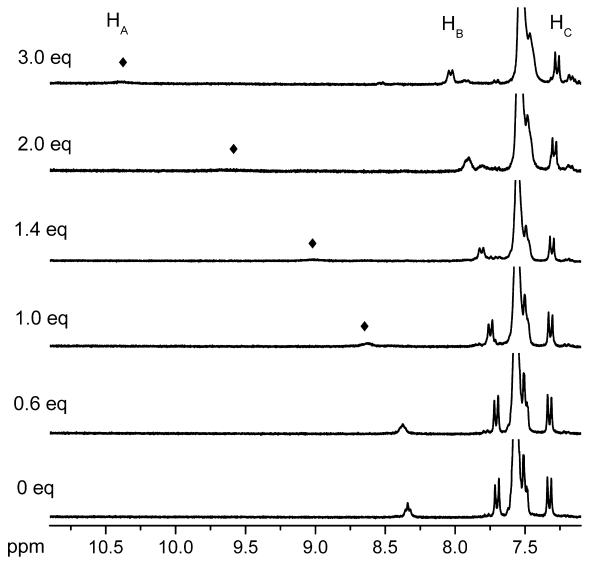

Figure 6. ^{1}H NMR spectral changes of **1c** (1.0 mmol dm^{-3}) in DMSO-d_6 upon addition of F^-.

The sensor molecule **1c** can interact selectively with both cations but also anions. Thus, it would be of interest to know whether it can act as a ditopic ion-pair sensor or not, which is expected to produce "cation-induced affinity", in which the anion binding abilities of a ditopic sensor could be enhanced in the presence of cations.[13d,28] To test this hypothesis, the ^{1}H NMR titration experiment was carried out. Figure S29 (Supporting Information) shows the spectral changes of **1c** (1.0 mmol dm^{-3}) in the presence of Ag^+ in DMSO-d_6 upon addition of F^-. Compared with the significant downfield shift of N−H and $-C_6H_4-$ motif signals when **1c** interacts with F^-, the signal changes are quite small here, which indicates the weak interaction between $[\mathbf{1c}\cdot Ag^+]$ and F^-. This observation is different from that in previous investigations that ditopic sensors bear "cation-induced affinity".[13d,28] Other anions could also not lead to the significant spectral changes in the presence of Ag^+ (for Cl^-, Br^-, I^-, $H_2PO_4^-$, and OAc^- see Figures S8−S10 and S30−S31 (Supporting Information), respectively). This behavior could be rationalized as the formation of a "closed clamp" conformation leading to the smaller space in tren cavity, which prevents $[\mathbf{1c}\cdot Ag^+]$ from anion-binding.

CONCLUSION

In summary, we reported the synthesis, photophysical properties and ion-sensing studies of novel tripodal gold(I) acetylide chemosensors **1c** and **1d**. Through a four-step reaction, **1c** and **1d** can be easily obtained. In THF and DMSO, **1c** and **1d** exhibit $\pi \rightarrow \pi^*$ absorption of the acetylide ligands. In the solid state and degassed THF solution, **1c** and **1d** show the $^3(\pi\pi^*)$ emission of acetylide ligands. Upon addition of Ag^+ into the DMSO solution of **1c** and **1d**, the $^3(\pi\pi^*)$ emission at 472 nm, which is not observed in the absence of Ag^+, was turned on and the emission color changed from blue-violet (very weak, DMSO background emission) to blue-green (strong). **1c** shows its higher selectivity and competitiveness for Ag^+ over other metal ions studied in this report. Through luminescence and UV−vis titration experiments, the binding constants of **1c** with Ag^+ (1:1) were determined to be 4.56 ± 0.21 (log K) and 4.35

dx.doi.org/10.1021/ic400791a | Inorg. Chem. XXXX, XXX, XXX−XXX

± 0.12 (log K'), respectively. The formation of the "closed clamp" conformation adduct [**1c**·Ag^+] was confirmed by ^{1}H NMR titration experiments. The receptor chelating effect of three-armed flexible conformation and the acetylide binding unit was determined by the control experiments toward the acetylide free analogue **1a** and single-arm analogue **2c**, respectively. The P(2-Py)Ph_2 containing analogue **1d** shows similar affinity but less selectivity toward Ag^+. In addition, **1c** shows the binding affinity toward F^- in DMSO-d_6 compared to other anions. In the presence of Ag^+, **1c** shows less binding affinity toward F^-. This could be rationalized by the smaller space in tren cavity when the "closed clamp" conformation adduct [**1c**·Ag^+] is formed. The study for water-soluble gold(I) acetylide chemosensors is underway.

■ ASSOCIATED CONTENT

Ⓢ Supporting Information

Synthetic route of **2c**; UV−vis and emission spectra of **1c** and **1d**; photophysical data of **1a**−**1d** and **2a**−**2c**; emission spectral changes of **1d** and **2c** with Ag^+; plots of the emission changes of **1c** and **1d** as a function of the concentration of Ag^+ and the theoretical 1:1 fitting curves; detection limit of **1c** toward Ag^+; emission spectra of **1c** and **1d** with metal ions; ^{1}H NMR spectral changes of **1c** in present of one equivalent of Ag^+ with F^-, Cl^-, Br^-, I^-, $H_2PO_4^-$, and OAc^-; ^{1}H NMR spectral changes of **1a**, **1b**, and **1d** with Ag^+; UV−vis spectral changes of **1d** with Ag^+; a Job's plot of **1d** with Ag^+; a plot of the absorbance change of **1d** as a function of the concentration of Ag^+ and a 1:1 theoretical fitting curve; emission spectra of **1c** in THF and DMSO with 2 equiv of Ag^+; UV−vis and emission spectral changes of **1c** with Cu^+; excitation spectra of **1c** with 4 equiv of Ag^+ and Cu^+; emission spectral changes of **1d** with Ag^+; ^{1}H NMR spectral changes of **1c** with Cl^-, $H_2PO_4^-$, and OAc^-. This material is available free of charge via the Internet at http://pubs.acs.org.

■ AUTHOR INFORMATION

Corresponding Author

*Phone: +86-20-84110062. Fax: +86-20-84112245. E-mail: zhaoxy@mail.sysu.edu.cn.

Notes

The authors declare no competing financial interest.

■ ACKNOWLEDGMENTS

We acknowledge the financial support from the National Natural Science Foundation of China (20971131 and J1103305), the Natural Science Foundation of Guangdong Province (10151027501000048 and S2012010010566), and Sun Yat−Sen University. We thank Prof. David G. Churchill of KAIST for his assistance in proofreading this manuscript. We also thank the editors and reviewers for their helpful comments and suggestions.

■ REFERENCES

(1) Valeur, B. *Molecular Fluorescence: Principle and Applications*; Wiley−VCH Verlag GmbH: Weinheim, 2001.

(2) Fu, F.; Wang, Q. *J. Environ. Manage.* **2011**, *92*, 407−418.

(3) Ratte, H. T. *Environ. Toxicol. Chem.* **1999**, *18*, 89−108.

(4) Zhang, J. F.; Zhou, Y.; Yoon, J.; Kim, J. S. *Chem. Soc. Rev.* **2011**, *40*, 3416−3429.

(5) (a) Zheng, H.; Yan, M.; Fan, X. X.; Sun, D.; Yang, S. Y.; Yang, L. J.; Li, J. D.; Jiang, Y. B. *Chem. Commun.* **2012**, *48*, 2243−2245. (b) Kim, J. M.; Lohani, C. R.; Neupane, L. N.; Choi, Y.; Lee, K. H. *Chem. Commun.* **2012**, *48*, 3012−3014. (c) Chatterjee, A.; Santra, M.; Won, N.; Kim, S.; Kim, J. K.; Bin Kim, S.; Ahn, K. H. *J. Am. Chem. Soc.* **2009**, *131*, 2040. (d) Coskun, A.; Akkaya, E. U. *J. Am. Chem. Soc.* **2005**, *127*, 10464−10465. (e) Yang, R. H.; Chan, W. H.; Lee, A. W. M.; Xia, P. F.; Zhang, H. K.; Li, K. A. *J. Am. Chem. Soc.* **2003**, *125*, 2884−2885. (f) Qin, C. J.; Wong, W. Y.; Wang, L. X. *Macromolecules.* **2011**, *44*, 483−489. (g) Bilgicli, A. T.; Gunsel, A.; Kandaz, M.; Ozkaya, A. R. *Dalton Trans.* **2012**, *41*, 7047−7056.

(6) (a) Mandal, A.; Dandapat, A.; De, G. *Analyst* **2012**, *137*, 765−772. (b) Gattas-Asfura, K. A.; Leblanc, R. M. *Chem. Commun.* **2003**, 2684−2685.

(7) (a) Feng, D. Q.; Liu, G. L.; Zheng, W. J.; Liu, J.; Chen, T. F.; Li, D. *Chem. Commun.* **2011**, *47*, 8557−8559. (b) Jagerszki, G.; Grun, A.; Bitter, I.; Toth, K.; Gyurcsanyi, R. E. *Chem. Commun.* **2010**, *46*, 607−609.

(8) (a) Xie, W. Y.; Huang, W. T.; Li, N. B.; Luo, H. Q. *Chem. Commun.* **2012**, *48*, 82−84. (b) Park, K. S.; Lee, J. Y.; Park, H. G. *Chem. Commun.* **2012**, *48*, 4549−4551. (c) Tang, C. X.; Bu, N. N.; He, X. W.; Yin, X. B. *Chem. Commun.* **2011**, *47*, 12304−12306. (d) Zhao, C.; Qu, K.; Song, Y.; Xu, C.; Ren, J.; Qu, X. *Chem.—Eur. J.* **2010**, *16*, 8147−8154. (e) Li, T.; Shi, L. L.; Wang, E. K.; Dong, S. J. *Chem.—Eur. J.* **2009**, *15*, 3347−3350. (f) Wen, Y.; Xing, F.; He, S.; Song, S.; Wang, L.; Long, Y.; Li, D.; Fan, C. *Chem. Commun.* **2010**, *46*, 2596−2598. (g) Man, B. Y. W.; Chan, D. S. H.; Yang, H.; Ang, S. W.; Yang, F.; Yan, S. C.; Ho, C. M.; Wu, P.; Che, C. M.; Leung, C. H.; Ma, D. L. *Chem. Commun.* **2010**, *46*, 8534−8536.

(9) Zhao, Q.; Li, F.; Huang, C. *Chem. Soc. Rev.* **2010**, *39*, 3007−3030.

(10) (a) Yam, V. W. W.; Cheng, E. C. C. *Chem. Soc. Rev.* **2008**, *37*, 1806−1813. (b) Yam, V. W. W.; Cheng, E. C. C. *Top. Curr. Chem.* **2007**, *281*, 269−309. (c) Pyykko, P. *Angew. Chem., Int. Ed.* **2004**, *43*, 4412−4456.

(11) (a) Tong, G. S. M.; Kui, S. C. F.; Chao, H. Y.; Zhu, N.; Che, C. M. *Chem.—Eur. J.* **2009**, *15*, 10777−10789. (b) Che, C. M.; Lai, S. W. *Coord. Chem. Rev.* **2005**, *249*, 1296−1309. (c) Zhang, H. X.; Che, C. M. *Chem.—Eur. J.* **2001**, *7*, 4887−4893. (d) Fu, W. F.; Chan, K. C.; Cheung, K. K.; Che, C. M. *Chem.—Eur. J.* **2001**, *7*, 4656−4664. (e) Fu, W. F.; Chan, K. C.; Miskowski, V. M.; Che, C. M. *Angew. Chem., Int. Ed.* **1999**, *38*, 2783−2785. (f) Yip, J. H. K.; Prabhavathy, J. *Angew. Chem., Int. Ed.* **2001**, *40*, 2159−2162.

(12) (a) Lee, T. K. M.; Zhu, N.; Yam, V. W. W. *J. Am. Chem. Soc.* **2010**, *132*, 17646−17648. (b) Yu, S. Y.; Sun, Q. F.; Lee, T. K. M.; Cheng, E. C. C.; Li, Y. Z.; Yam, V. W. W. *Angew. Chem., Int. Ed.* **2008**, *47*, 4551−4554. (c) Sun, Q. F.; Lee, T. K. M.; Li, P. Z.; Yao, L. Y.; Huang, J. J.; Huang, J.; Yu, S. Y.; Li, Y. Z.; Cheng, E. C. C.; Yam, V. W. W. *Chem. Commun.* **2008**, 5514−5516. (d) Yu, S. Y.; Zhang, Z. X.; Cheng, E. C. C.; Li, Y. Z.; Yam, V. W. W.; Huang, H. P.; Zhang, R. B. *J. Am. Chem. Soc.* **2005**, *127*, 17994−17995.

(13) (a) Zhou, Y. P.; Zhang, M.; Li, Y. H.; Guan, Q. R.; Wang, F.; Lin, Z. J.; Lam, C. K.; Feng, X. L.; Chao, H. Y. *Inorg. Chem.* **2012**, *51*, 5099−5109. (b) He, X.; Zhu, N.; Yam, V. W. W. *Dalton Trans.* **2011**, *40*, 9703−9710. (c) Hau, F. K. W.; He, X.; Lam, W. H.; Yam, V. W. W. *Chem. Commun.* **2011**, *47*, 8778−8780. (d) He, X.; Yam, V. W. W. *Inorg. Chem.* **2010**, *49*, 2273−2279. (e) He, X.; Herranz, F.; Cheng, E. C. C.; Vilar, R.; Yam, V. W. W. *Chem.—Eur. J.* **2010**, *16*, 9123−9131. (f) He, X.; Lam, W. H.; Zhu, N.; Yam, V. W. W. *Chem.—Eur. J.* **2009**, *15*, 8842−8851. (g) He, X.; Cheng, E. C. C.; Zhu, N.; Yam, V. W. W. *Chem. Commun.* **2009**, 4016−4018. (h) Li, C. K.; Lu, X. X.; Wong, K. M. C.; Chan, C. L.; Zhu, N.; Yam, V. W. W. *Inorg. Chem.* **2004**, *43*, 7421−7430.

(14) (a) Tong, G. S. M.; Chow, P. K.; Che, C. M. *Angew. Chem., Int. Ed.* **2010**, *49*, 9206−9209. (b) Lu, W.; Zhu, N.; Che, C. M. *J. Organomet. Chem.* **2003**, *670*, 11−16. (c) Lu, W.; Xiang, H. F.; Zhu, N.; Che, C. M. *Organometallics.* **2002**, *21*, 2343−2346. (d) Chao, H. Y.; Lu, W.; Li, Y.; Chan, M. C. W.; Che, C. M.; Cheung, K. K.; Zhu, N. *J. Am. Chem. Soc.* **2002**, *124*, 14696−14706. (e) Che, C. M.; Chao, H. Y.; Miskowski, V. M.; Li, Y.; Cheung, K. K. *J. Am. Chem. Soc.* **2001**, *123*, 4985−4991.

(15) (a) Rathore, R.; Chebny, V. J.; Abdelwahed, S. H. *J. Am. Chem. Soc.* **2005**, *127*, 8012−8013. (b) Kang, J.; Choi, I.; Kwon, J. Y.; Lee, E. Y.; Yoon, J. *J. Org. Chem.* **2002**, *67*, 4384−4386.
(16) Yam, V. W. W.; Cheung, K. L.; Cheng, E. C. C.; Zhu, N.; Cheung, K. K. *Dalton Trans.* **2003**, 1830−1835.
(17) Tang, H. S.; Zhu, N.; Yam, V. W. W. *Organometallics.* **2007**, *26*, 22−25.
(18) (a) Lam, E. S. H.; Tam, A. Y. Y.; Lam, W. H.; Wong, K. M. C.; Zhu, N.; Yam, V. W. W. *Dalton Trans.* **2012**, *41*, 8773−8776. (b) Koshevoy, I. O.; Lin, C. L.; Karttunen, A. J.; Janis, J.; Haukka, M.; Tunik, S. P.; Chou, P. T.; Pakkanen, T. A. *Inorg. Chem.* **2011**, *50*, 2395−2403. (c) Wei, Q. H.; Zhang, L. Y.; Yin, G. Q.; Shi, L. X.; Chen, Z. N. *J. Am. Chem. Soc.* **2004**, *126*, 9940−9941.
(19) Yam, V. W. W.; Wong, K. M. C. *Top. Curr. Chem.* **2005**, *257*, 1−32.
(20) (a) Arunachalam, M.; Ghosh, P. *Chem. Commun.* **2011**, *47*, 8477−8492. (b) Mullen, K. M.; Beer, P. D. *Chem. Soc. Rev.* **2009**, *38*, 1701−1713.
(21) Ravikumar, I.; Ghosh, P. *Chem. Soc. Rev.* **2012**, *41*, 3077−3098.
(22) (a) Busschaert, N.; Wenzel, M.; Light, M. E.; Iglesias-Hernandez, P.; Perez-Tomas, R.; Gale, P. A. *J. Am. Chem. Soc.* **2011**, *133*, 14136−14148. (b) Berezin, S. K.; Davis, J. T. *J. Am. Chem. Soc.* **2009**, *131*, 2458.
(23) Uson, R.; Laguna, A.; Laguna, M. *Inorg. Synth.* **1989**, *26*, 85−91.
(24) Churchill, D. G. *J. Chem. Educ.* **2006**, *83*, 1798−1803.
(25) (a) Bourson, J.; Pouget, J.; Valeur, B. *J. Phys. Chem.* **1993**, *97*, 4552−4557. (b) Mo, H. J.; Shen, Y.; Ye, B. H. *Inorg. Chem.* **2012**, *51*, 7174−7184.
(26) (a) Gomez, D. E.; Fabbrizzi, L.; Licchelli, M.; Monzani, E. *Org. Biomol. Chem.* **2005**, *3*, 1495−1500. (b) Esteban-Gomez, D.; Fabbrizzi, L.; Liechelli, M. *J. Org. Chem.* **2005**, *70*, 5717−5720. (c) Boiocchi, M.; Del Boca, L.; Esteban-Gomez, D.; Fabbrizzi, L.; Licchelli, M.; Monzani, E. *Chem.—Eur. J.* **2005**, *11*, 3097−3104. (d) Boiocchi, M.; Del Boca, L.; Gomez, D. E.; Fabbrizzi, L.; Licchelli, M.; Monzani, E. *J. Am. Chem. Soc.* **2004**, *126*, 16507−16514.
(27) Ravikumar, I.; Lakshminarayanan, P. S.; Ghosh, P. *Inorg. Chim. Acta* **2010**, *363*, 2886−2895.
(28) (a) Mahoney, J. M.; Stucker, K. A.; Jiang, H.; Carmichael, I.; Brinkmann, N. R.; Beatty, A. M.; Noll, B. C.; Smith, B. D. *J. Am. Chem. Soc.* **2005**, *127*, 2922−2928. (b) Mahoney, J. M.; Beatty, A. M.; Smith, B. D. *Inorg. Chem.* **2004**, *43*, 7617−7621. (c) Mahoney, J. M.; Beatty, A. M.; Smith, B. D. *J. Am. Chem. Soc.* **2001**, *123*, 5847−5848.

dx.doi.org/10.1021/ic400791a | *Inorg. Chem.* XXXX, XXX, XXX−XXX